IN-SITU CURE MONITORING OF 3D WOVEN COMPOSITES WITH A MULTIFUNCTIONAL CNT SENSOR

Dilan Arslan[1], Melisa Dincer[2], Zeynep N. Akyazici[3], Eyuphan Kucukkalfa[4], Elif R. Demirer[5], Kaan Yildiz[6], Basak Ozkendirci[7], Elif Ozden-Yenigun[8], and Hulya Cebeci[9]

[1] Department of Chemistry, Istanbul Technical University, Istanbul, Turkiye, arslan22@itu.edu.tr,
[2] Aviation Institute, Istanbul Technical University, Istanbul, Turkiye, dincer18@itu.edu.tr,
[3] Department of Aeronautical and Astronautical Engineering, Istanbul Technical University, Istanbul, Turkiye, akyazici15@itu.edu.tr,
[4] Aviation Institute, Istanbul Technical University, Istanbul, Turkiye, kucukkalfa16@itu.edu.tr,
[5] Aerospace Research Center, Istanbul Technical University, Istanbul, Turkiye, demirere18@itu.edu.tr,
[6] Aviation Institute, Istanbul Technical University, Istanbul, Turkiye, yildizkaa@itu.edu.tr,
[7] Faculty of Arts and Design, Department of Textile and Fashion Design, Dogus University, Istanbul, Turkiye, bozkendirci@dogus.edu.tr,
[8] School of Design Textiles, Royal College of Art, London, United Kingdom, elif.ozden-yenigun@rca.ac.uk,
[9] Department of Aeronautical and Astronautical Engineering, Istanbul Technical University, Istanbul, Turkiye, geyikh@itu.edu.tr

Keywords: Structural health monitoring, Cure monitoring, 3D woven orthogonal

ABSTRACT

In-situ process monitoring is essential in defining optimal composite production procedures by tracking resin flow and cure kinetics. Due to their piezoresistive properties, it is possible to monitor such processes and deformations in composites by integrating carbon nanotubes (CNTs) into structures. Hence, incorporating CNTs dispersions into any surface can be utilized as strain sensors. The dispersion of CNTs can be improved by combining them with other nanomaterials, such as cellulose nanocrystals (CNCs). The CNTs:CNCs dispersion can be applied to fabrics for deformation detection applications using screen printing technology. Here, the CNTs:CNCs dispersion was screen printed onto 3D woven orthogonal fabrics as multi-sensors for both cure monitoring and followed by strain measurements under compressive loading. The conductive dispersions of CNTs:CNCs were initially studied for the rheology and stability at various CNTs to CNCs ratios. The print quality, thickness, and pattern effect have been investigated for the performance of CNTs:CNCs sensors, and for a two-layered sensor printing, the resistance was decreased by 73% compared to single-layered, meaning that the electrical conductivity was improved. Moreover, compression sensing was analyzed, and the curing degree was calculated as -9.3×10^{-6} °C^{-1}.

1 INTRODUCTION

Non-destructive testing (NDT) techniques are frequently utilized in applications, including inspecting composite manufacturing processes to evaluate product quality and detecting damage mechanisms during the service life [1]. Besides, damage sensing capabilities of materials intended for use in sensor applications can be investigated by NDT. However, the offline conventional NDT systems impose stringent requirements on reliability and safety against the possibility of unexpected failure, which conflict with the design concept of lightness. Demand for in-situ integrated structural health monitoring (SHM) systems has increased instead of offline non-destructive testing methods to reduce the risk of severe failures [2]. In-situ monitoring contributes to efficient production, particularly in composite production methods such as the vacuum infusion method, where resins are utilized by tracking the resin flow characteristics and curing kinetics. Thus, the composite material with ideal mechanical properties can be manufactured by inspecting the resins' exact curing time and gelling time under various ambient temperatures.

The favorable approaches to bring a deformation detection capability to the composite materials are

integrating fiber optic sensors, nanomaterials based on smart piezoelectric films, or coatings. Carbon nanotubes (CNTs) can be a great alternative to detect deformation in SHM studies considering their high mechanical, thermal, and electrical properties and piezoresistive response [3,4]. Labiano et al. stated that CNTs dispersions could be integrated into surfaces of fabrics to be utilized as strain sensors and antennas. However, due to their hydrophobic behavior, CNTs are prone to agglomerate and obstruct their dispersion in solvents. To prevent CNTs from generating strong Van der Waals bonds with each other and to create a more uniform dispersion in distilled water, other nanomaterials, such as cellulose nanocrystals (CNCs), can be combined. Given the chemical nature of CNCs, their hydrophilic parts, which can bond with distilled water, and their nonpolar parts, which can bond with CNTs, enable them to provide colloidal stability [5]. As a result, CNTs:CNCs dispersion in distilled water can be prepared and applied to fabrics for deformation detection applications.

Transferring CNTs:CNCs dispersions to the fabrics can be performed by screen printing, a versatile process capable of dispersion printing on substrates such as fabrics, plastics, and metals [6], [7]. Conductive dispersions consist of materials with high electrical conductivity and can be applied through screen printing to achieve a uniform and homogeneous distribution on substrates which enables the creation of low-resistance connections and circuits [8], [9]. Moreover, conductive dispersion-based sensors are also lightweight and portable. Cure monitoring of sensors with conductive dispersions ensures proper curing and optimization of their performance. Cure monitoring involves controlling the curing or hardening process of the conductive inks applied to the sensors. This ensures that the sensors are properly cured and achieve the desired properties and functionality. Real-time monitoring of optimal conditions and ensuring uniformity across multiple prints or batches. Recently, several researchers have used CNTs-based sensors for the cure monitoring of a composite during the manufacturing process. Luo et al. improved the SWCNT-FibSen which is a single-walled carbon nanotube thin-film 1D fiber sensor, with a continuous spray coating and winding method, with glass, polyaramid, nylon, and polyethylene terephthalate as the fiber substrate [10]. Lu et al. developed a bucky paper (BP) consisting of multi-walled carbon nanotubes (MWCNTs) by spray-vacuum filtration method [11]. This fabricated flexible and sensitive carbon nanotube bucky paper (MWCNTs-BP) sensor could monitor the dynamic fabrication process of fiber-reinforced composites in real time and be integrated into complex curved surfaces and critical stress areas. Moreover, Dai et al. deposited CNTs on a nonwoven textile to create a thin and porous field sensor and developed a new multifunctional sensor [12]. Therefore, examining curing through sensors integrated into surfaces such as fabrics helps understand the appropriate curing cycles and degrees.

Conventional polymer matrix composites consisting of 2D fabric layers have been used in many applications, but 3D woven orthogonal fabrics gain importance with their higher impact tolerance and fracture toughness properties [13]. Moreover, 3D woven orthogonal fabrics offer a solution to eliminating the delamination problem by the yarns that mutually orthogonal directions. By embedding or printing the sensors in the 3D woven orthogonal fabric, the ability to monitor phase transformations during the gelation and vitrification can be gained, which composite manufacturing processes need further assessments for 3D structures. In addition, the dissimilarity in the thermochemical properties between the resin and fiber is induced by residual stresses that cause deformations. Monitors the cure of 3D woven orthogonal fabrics, providing a better explanation of curing process-induced deformations that occur when the fabric is thicker [14–17].

In here, the demonstration of in-situ cure and strain monitoring has been performed by printed multi-sensor composites of CNTs:CNCs on 3D woven orthogonal composites. A custom-built weaving machine established the 3D weaving process, and 3D woven orthogonal fabrics from glass fibers were fabricated. The conductive dispersions of CNTs:CNCs were initially studied for the rheology and stability at CNTs:CNC ratios of 1:2, 2:1, and 1.5:1.5. The screen-printing process has been simulated for the viscosity exploration and the CNTs:CNCs resulted as the optimum condition. The print quality, thickness, and pattern effect have been investigated for the performance of CNTs:CNCs sensors, and for a two-layered sensor printing, the resistance was decreased by 73% compared to single-layered, meaning that the electrical conductivity was improved. Moreover, compression sensing was examined and the curing degree was calculated as -9.3×10^{-6} $°C^{-1}$.

2 MATERIALS AND METHODS

2.1. Materials

CNTs were purchased from Nanocyl (Sambreville, Belgium) with a purity of 90%, an outer diameter of 9.5 nm, and a length of 1.5 µm. CNCs were provided from CelluForce, (Windsor, QC, Canada), with a diameter of 2.3–4.5 nm and an average length of 44–108 nm [18]. The silver paste was purchased from Nanografi (Ankara, Turkiye). A K-type thermometer (UT 325) was purchased from Unit (Kocaeli, Turkiye). 300 TEX E-glass fibers supplied by SISECAM, (Istanbul, Turkiye). Screen printing was performed using a polyurethane squeegee and a 26×32 cm wooden silk frame with a mesh size of 55 thread/cm (55T) (Bitti Gitti, Istanbul, Turkiye). The epoxy resin/hardener system was purchased from CET Composite (Istanbul, Turkiye) and mixed with a 100:27 epoxy:hardener weight ratio. The epoxy resin (CE-A 1546) has a 1200-1400 mPas viscosity and 1.1-1.2 g/cm^3 density at 25°C, while the curing agent (CE-B 10560) has 300-450 mPas viscosity and 0.95-1 g/cm^3 density at 25 °C. All chemicals were used as received.

2.2. Preparation of Orthogonal Fabrics

3-Dimensional woven orthogonal fabrics (3D-ORT) were produced using E-glass fibers (GF), with a linear density of 300 TEX. The 3-Dimensional orthogonal weaving process was performed in a semi-automated custom-built weaving machine to obtain a standard yarn density throughout the fabric. The 3D-ORT fabric was made of yarns interlaced to each other and oriented in an orthogonal direction: the warp yarns along the length of the fabric, the weft yarns inserted in the perpendicular direction between the warp yarns, and the z-yarns that bounded the wefts and the warps yarns in the thickness direction. To optimize the woven fabric surface, preliminary experiments included screen printing of CNTs:CNCs dispersion on 3D orthogonal woven fabrics. Results show that it is necessary to print the CNTs:CNCs ink on the 3D orthogonal woven fabric as a flat surface for preserving the conductive pattern. Consequently, 300 TEX yarns were employed to achieve a tight structure and print the CNTs:CNCs dispersions as flat as possible on the fabric's surface. Initially, the modeling has been performed to weave the 3D orthogonal woven fabric, as presented in Fig. 1a, by TEXGEN software.

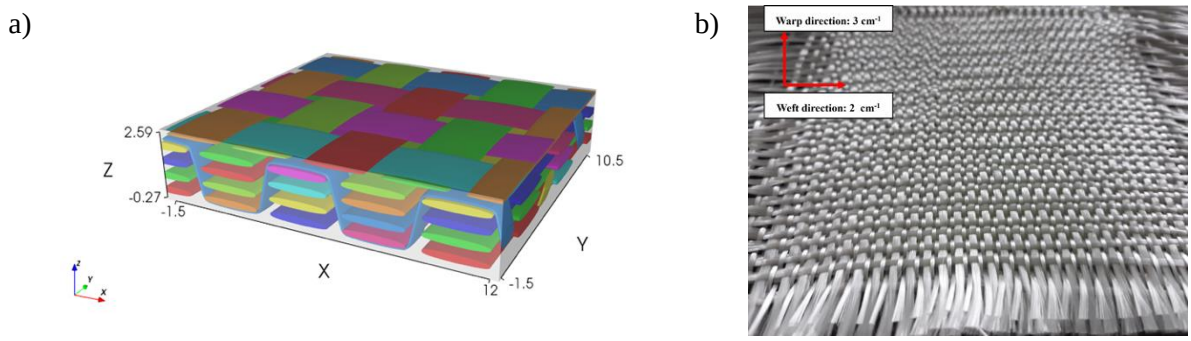

Figure 1: a) Modeling of 3D orthogonal woven fabric, b) 3D orthogonal woven fabric

The 3D orthogonal fabric was woven by providing sufficient tightness with a warp density of 3 cm^{-1} and a weft density of 2 cm^{-1} as a plain pattern. The z-yarn to warp yarn ratio was chosen as 1:1, and this woven structure was designed with four layers, as shown in Fig. 1b. The plain pattern of 3D woven fabric facilitated the flat patterning of CNTs:CNCs dispersions on the top layer were provided tightly to the structure and simplified the flat patterning of CNTs:CNCs ink dispersion.

2.3. Preparation of CNTs:CNCs Dispersions

The first step of CNTs:CNCs inks was to disperse the CNCs into deionized water (DI-H_2O), followed by stirring for 15 minutes at 700 rpm using a magnetic stirrer at the requested amount. Subsequently,

the CNCs:DI-H_2O dispersion was subjected to ultrasonic treatment for 15 minutes at 20 kHz, 23 watts, and 30% amplitude using a probe sonicator (Sonics VCX750). As mentioned earlier, CNTs were added to the dispersion to generate inks containing 3% by weight of CNTs:CNCs and continued the sonication with the same procedure for 1 hour. The proportions of 2:1, 1:2, and 1.5:1.5 for CNTs:CNCs were formulated following similar steps, and all content is summarized in

Dispersions	CNTs (wt. %)	CNCs (wt. %)
CNTs:CNCs-1:2	1	2
CNTs:CNCs-1.5:1.5	1.5	1.5
CNTs:CNCs-2:1	2	1

Table 1:Dispersions of CNTs:CNCs at various concentrations.

2.4. Screen Printing of 3D Orthogonal Woven Fabric

Initially, for achieving adequate adhesion of CNTs:CNCs dispersions on the glass fiber surface, the sizing of the glass fiber was removed at an acetone bath under sonication. However, the results were not promising for the screen printing process due to hydrophobicity; hence all CNTs:CNCs dispersions were directly printed on woven fabrics without post-treatment. A manual screen printing setup was used to print conductive CNTs:CNCs-1:2, CNTs:CNCs-1.5:1.5, and CNTs:CNCs-2:1 dispersions as two layers on 20 mm x 70 mm samples as presented in Fig. 2. The pattern was selected on its electrical sensitivity with its unique geometry having a two times higher elongation at the y-axis.

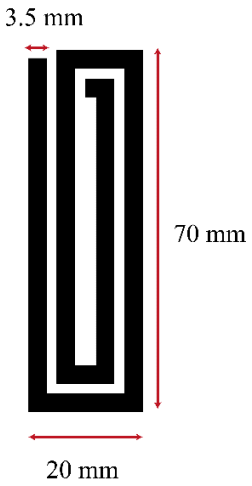

Figure 2: Design of the screen-printed pattern.

Each sample and layer were screens printed under the same conditions to achieve comparable results. 1 mL of dispersion was dropped into the screen-printing mold, and ten layers were printed to obtain a uniform and homogeneous pattern. Under the same conditions, using formulated dispersions, two printing layers were deposited on the orthogonal 3D woven fabric. Resistance values of samples were measured with Keithley at each layer, as detailed in Section 3.3.

2.5. Composite Manufacturing Process

The CNTs:CNCs-printed 3D woven fabrics were infused with epoxy through a vacuum infusion process, and curing was performed at a membrane table as HEATCON has a thoroughly vacuumed environment and controllable heating at a rate of 10 °C/min. Peel-ply, infusion mesh, and vacuum bag were placed on the 3D woven fabric, where the vacuum-infusion process was applied on a glass plate, as demonstrated in Fig. 3 (created with Chemix). Furthermore, copper wires were stuck on the materials via silver paste to measure resistance change and a thermocouple was utilized to investigate the curing and cooling cycle of the resin. Keithley was used to monitor the resistance change during the composite manufacturing process. Finally, the resin was infused, and two curing procedures were examined: 24 hours at room temperature and 2 hours at 100 °C, according to the manufacturer's instructions.

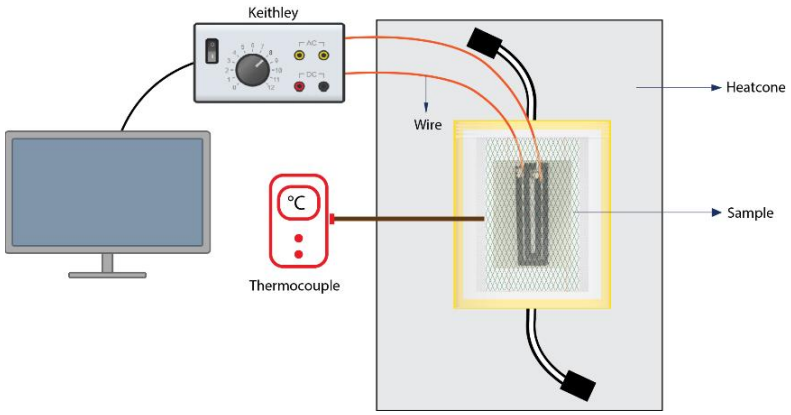

Figure 3: Schematic of the experimental setup for the composite manufacturing process.

3 CHARACTERIZATION

3.1 Rheological Behaviors

The rheological properties of the CNTs:CNCs dispersions were characterized using a rotational rheometer (TA Instruments Discovery Hybrid Rheometer 2) equipped with parallel plates of 25 mm radius and a 1 mm gap distance. The tests were performed at room temperature and repeated three times to ensure reproducibility. Before starting all the rheological tests, the conductive dispersions were pre-sheared at 1.0 s^{-1} for 20 s. The shear viscosity of conductive dispersions plays a significant role in screen printing. Thus, the steady-state rheological step test was carried out in a shear rates range of 0.1-1000 s^{-1}.

3.2 Rheological Behavior During the Printing Simulation

During the printing process, the dispersion undergoes non-constant shear rates, leading to damage and recovery of its structure, known as thixotropy. To better understand the dispersion's rheological behavior during printing, a simulation was conducted that involved applying a shear rate of 0.1 s^{-1} for 60 seconds before the squeegee operation, a shear rate of 100 s^{-1} for 50 seconds during the squeegee operation to simulate the printing process, and a shear rate of 0.1 s^{-1} for 180 seconds after the squeegee operation [19]. The recovery rate of all dispersions at the 120th second was calculated.

3.3 Electrical Characterization

The electrical resistance of conductive surfaces was measured in a two-point probe configuration from current and voltage measurements generated using a Keithley 2400 source meter interfaced with a computer running LabVIEW software. The LabVIEW program was such that a voltage of between -5.0 and 5.0 was sourced from the Keithley source meter to the conductive pattern, and then the current across it was measured. Resistance values were obtained from the slope of the resulting current-voltage

(I-V) graph. For each sample, three measurements were performed by varying sites on the surface; the mean resistances were reported in section 4.3.

The resistance change of fabrics during the vacuum infusion process of resin and compression test with balance calibration weights were measured by a Keithley 2400 source meter/LabVIEW software. Copper wires with crocodile clips were connected, and silver paste was glued to the printed conductive pattern on a 3D-ORT. During the compression test, 50g, 100g, and 500g of calibration weights were applied to the cured samples for 15-second repetitions, and change in resistance were measured.

4. RESULTS

4.1 Rheological Behaviors

The rheology of the dispersions is crucial for the success of a screen-printed pattern, especially when thinner lines and sharper edges are present. The degree of particle distribution in the CNTs:CNCs dispersions were affected by various parameters, including the solvent system and solid content, which resulted in various rheological behaviors. The viscosities of the CNTs:CNCs dispersion compositions with different weight ratios were evaluated using a plate rheometer, and results were presented and tabulated as a function of frequency in Fig. 4 and Table 2.

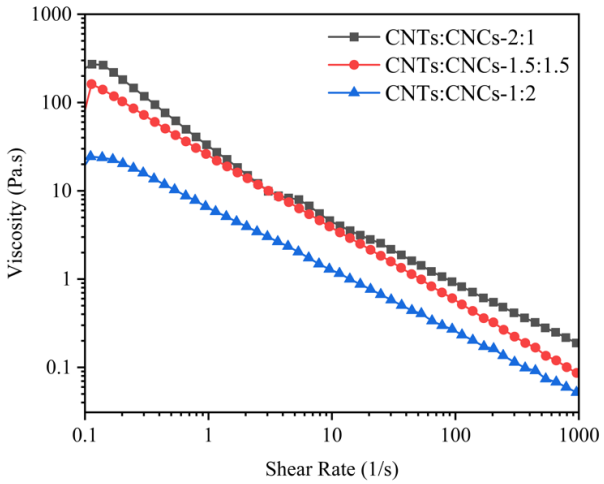

Figure 4: Shear viscosity of CNTs:CNCs-based dispersions versus shear rate.

All inks showed shear-thinning behavior at a frequency of 10^{-1} to 10^{3} s^{-1}. Additionally, the viscosity was enhanced with the increasing CNTs content in the dispersion. Shear forces enabled the breaking of CNTs clusters and aligned particles along the flow direction, resulting in the sliding of smaller CNTs clusters and a shear-thinning profile. In screen printing, shear stress between the squeegees assisted in lowering dispersion viscosity, which was advantageous to the dispersion's smooth transfer.

	Viscosity (Pa.s)			
Shear Rates / Ink Composition	0.1 s^{-1}	1.0 s^{-1}	10 s^{-1}	100 s^{-1}
CNTs:CNCs-1:2	18 ± 2	4.5 ± 0.7	0.9 ± 0.1	0.9 ± 0.01
CNTs:CNCs-1.5:1.5	214 ± 23	32.5 ± 2.3	5.2 ± 0.3	1.1 ± 0.05
CNTs:CNCs-2:1	335 ± 11	53.0 ± 4.0	7.7 ± 0.2	1.3 ± 0.01

Table 2: Viscosities of CNTs:CNCs dispersions at 1:2, 2:1, and 1.5:1.5 as of shear rates.

4.2. Rheological Behavior During the Printing Simulation

Viscosity dropped sharply when the shear rate rose from 0.1 s^{-1} to 100 s^{-1} as seen in Fig. 5. Destroying the dispersion's structure with the shear stress might encourage the dispersion to flow smoothly through the mesh. The dispersion structure was rebuilt and restored once the shear rate dropped to 0.1 s^{-1}.

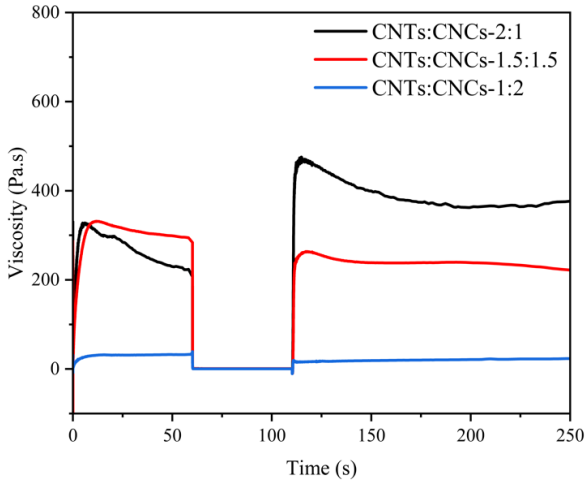

Figure 5: Viscosity behavior during the printing simulation.

With the lowest % recovery rate of 46%, CNTs:CNCs-1:2 had the lowest viscosity of 0.24 Pa.s at 100 s^{-1}, as seen in Fig. 6a. Hence, the dispersion was spread on the glass fiber surface during screen printing. However, CNTs:CNCs-2:1 possessed the highest viscosity of 0.90 Pa.s at 100 s^{-1} with a recovery rate of 174.06%. Although the recovery rate was high, the prints made with CNTs:CNCs-2:1 resulted in low capability flow through the meshes, as demonstrated in Fib. 6b. On the other hand, CNTs:CNCs-1.5:1.5 dispersion has a viscosity of 0.43 Pa.s with a recovery rate of 98.7% which was easily transferred to the surface of woven glass fiber Fig. 6c with high printing quality.

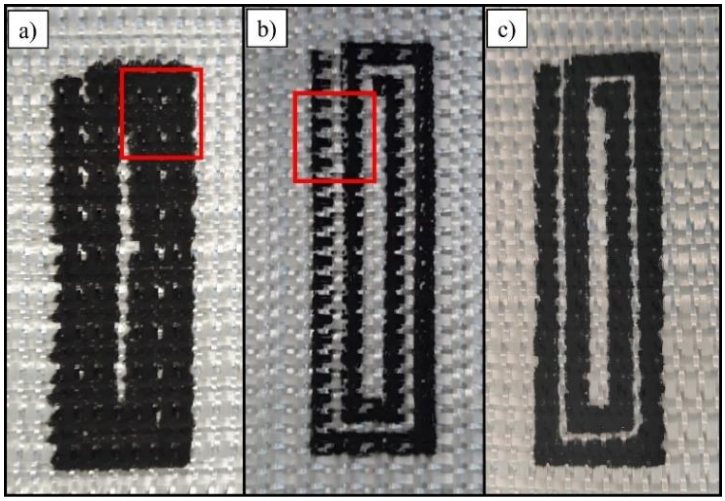

Figure 6: Screen printed orthogonal 3D woven fabrics a) CNTs:CNCs-1:2, b) CNTs:CNCs-2:1, and c) CNTs:CNCs-1.5:1.5 dispersions printed. The areas marked in red refer to unsuccessful prints on the 3D woven fabric.

4.3. Electrical Characterization of Printed Layers

The ohmic behavior of the fabricated sensors can be explained using I-V curves, which also show the formation of a stable conductive network. The ohmic behaviors of sensors with different layers were investigated to understand the formed conductive CNTs pathway. From the first to a second layer of printed CNTs onto woven GFs, the resistance values were decreased from 25.7±9.1 kΩ to 7.03±2.32 kΩ since with the second layer application, despite the 3D woven orthogonal fabrics, the voids were filled, and a more uniform sensor was formed as can be seen in Fig. 7.

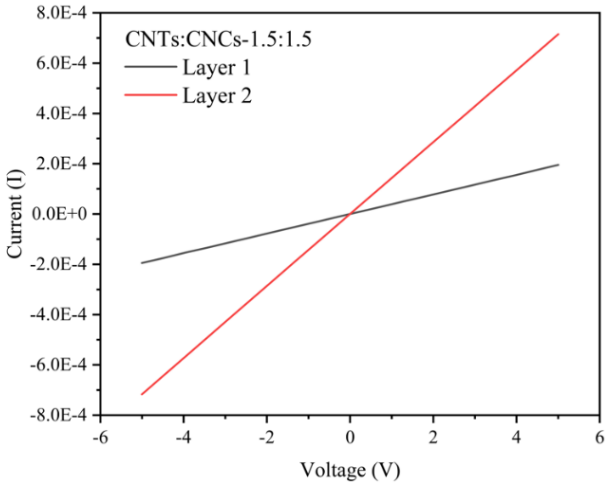

Figure 7: I-V curves of screen-printed sensor onto orthogonal 3D woven fabric.

4.4. Curing Process Monitoring with Screen-Printed Sensor

During the composite manufacturing process, continuous monitoring of the printed CNTs sensor's resistance change in real-time offers significant scientific insights into the progression of the resin curing process. Extensive estimation and compression of screen printed fiber sensor's sensing performance were conducted to achieve valuable insights into the in-situ monitoring of composite material and investigate the underlying relationship between structure and properties. This assessment collected real-time resistance change ($\Delta R/R_0$) data over 24 hours during the vacuum-assisted resin transfer molding process at ambient temperature. Upon initial examination of the experimental data presented in Fig. 8, it is evident that the resistance change of the sensor exhibits distinguished changes corresponding to epoxy resin flowing through the sensor. This succeeded for approximately 10 minutes, during which resistance change gradually approached and stabilized at peak value. Subsequently, as the process continues, $\Delta R/R_0$ demonstrates a substantial decline, gradually reaching a plateau for the remainder of the processing. Notably, resistance changes were 275% when epoxy resin started flowing on the sensor (Fig. 8a).

The resistance responses of CNTs:CNCs-1.5:1.5 sensors printed onto orthogonal 3D woven fabrics were observed throughout the distinct curing cycles, encompassing three sequential stages: (1) temperature ramping from 25 ℃ to 100 ℃; (2) isothermal heating at the predetermined temperature for a duration of 2 hours; (3) subsequent natural cooling to 40 ℃. Irrespective of the variances in the curing cycles employed, the real-time resistance variation of the CNTs:CNCs-1.5:1.5 printed sensor consistently and accurately captured the fundamental characteristics exhibited during each of the three sequential processing stages (Fig. 8b).

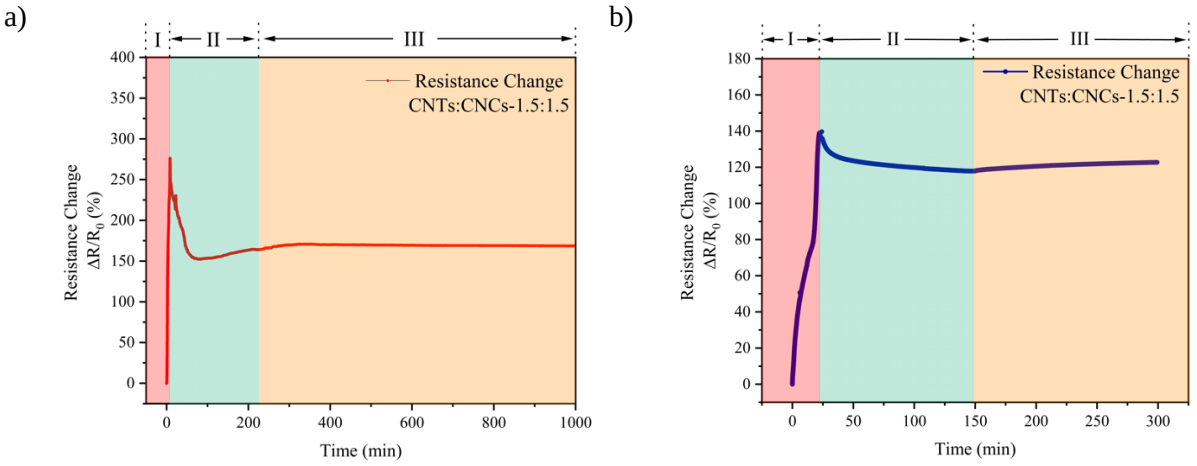

Figure 8: Temperature and relative resistance of cycle of in situ cure monitoring a) standard cure cycle at room temperature b) different three different cure cycles.

In the experiment's initial stage, the resin's prompt introduction was conducted to ensure complete saturation of the roving surface and complete filling of voids within the fabric structure. Concurrently, the resin molecules infiltrated and expanded the conductive network of CNTs, leading to significant alterations in the original structural configurations. These modifications increased tunneling distance and disruption of particle-to-particle contacts [20]. Subsequently, as the resin progressively filled most of the inter-roving voids, it underwent a relatively slower infiltration process within the micro- or nanoscaled spaces between individual rovings. As a result, the continuity of the conductive network experienced only minor disruptions during this phase (stage I). After the infusion stage, the electrical response during the stage is depicted in Fig. 8, the $\Delta R/R_0$ values of the sensor remained nearly constant once it reached its maximum values. This observation strongly suggests the cessation of resin flow, indicating that both the sensor and the surrounding resin entered a state of equilibrium (stage II). While the viscoelastic properties of the resin continued to evolve, the low viscosity and limited cross-linking structure did not significantly disturb the configuration of the sensing network. After the completion of the infusion stage, a noticeable decrease in resistance was observed in the sensors. This behavior can be attributed to the simultaneous occurrence of a substantial rise in viscosity and volumetric shrinkage during the gelation of resin, which leads to the closer proximity of conductive particles and pathways, thereby facilitating improved electron transport.

During the cooling stage (stage III), the temperature declined, and the resistance increased due to the intrinsic negative temperature coefficient (NTC) effect of the CNTs network [21]. While the thermal expansion of the fully cured composite could affect the sensor resistance during stage III, this contribution is deemed negligible, owing to the relatively small thermal expansion coefficient of the epoxy/glass composite after full curing [22].

4.5. Temperature Resistance Coefficient and Curing Degree

The curing process of composites leads to variations in the degree of cure, resulting in distinct temperature responses of the resin at different curing stages. Here, the temperature responses of the screen-printed sensor during the cooling stage (stage III) were exhibited. The concept of a temperature resistance coefficient (TCR) is introduced to address this. Establishing a definite TCR makes it possible to determine the degree of cure of a composite based on a specific law or relationship. The TCR quantifies the proportional variation in material resistance with respect to unit changes in temperature. It is mathematically represented by the following formula:

$$TCR = \Delta R/(R_0 \Delta T) \quad (1)$$

A reduced degree of cure results in a decreased cross-link density within the resin, rendering the entire resin network more responsive to temperature variations. In the presence of temperature changes, the relaxation of polymer chains within the resin network becomes more pronounced when the curing degree is lower [22]. The degree of cure in composites can be assessed by monitoring the TCR value during the curing process. Through modifications to the composite material's curing system, the TCR of the printed sensor was determined, leading to enhanced curing degrees and improved manufacturing quality of the composites. Specifically, a lower curing degree corresponded to a higher absolute value of TCR, indicating increased temperature sensitivity of embedded printed sensors within the composite material. Following the completion of the cooling stage, the TCR value corresponds to -9.2×10^{-6} °C^{-1}, which indicates that curing is complete.

4.6. Compression Test Behavior

To assess the stability of the investigated CNTs sensing materials, in-situ compression cyclic tests were conducted as a preliminary examination, simultaneously measuring the changes in electrical resistance. Samples were subjected to 50g, 200g, and 500g of weights for cyclic loading and unloading tests. Electromechanical responses of the CNTs sensing materials under different weights were exhibited in Fig. 9. It was observed that the cured composite material's resistance change decreased via 50g and 200g weights, and it was attributed to CNTs' connection within the conductive line. However, when the amount of stress was increased, the response became more regular. Still, resistance change increased, and we believe that this behavior originated from deformation in the structure of the composite and conductive line.

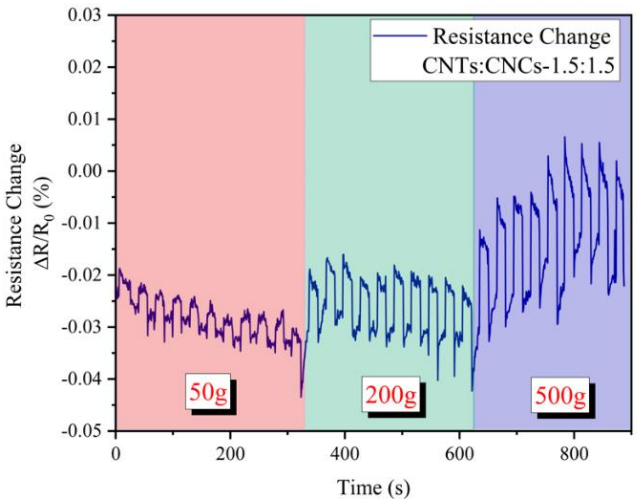

Figure 9: Resistance change versus weight of 50g, 200g, and 500g.

5 CONCLUSIONS

In conclusion, this study demonstrated the feasibility of in-situ cure monitoring and structural health monitoring utilization of a printed sensor, explicitly focusing on 3D woven orthogonal fabric. Firstly, the 3D woven orthogonal fabrics have been fabricated by a custom-built weaving machine. Then, the CNTs:CNCs dispersions have been developed. Subsequently, dispersions comprising CNTs and CNCs were developed, wherein incorporating CNCs improved dispersion uniformity. The CNTs:CNCs dispersion was then screen printed onto the 3D woven orthogonal fabrics using screen printing technology to investigate the sensor properties. The laminated composites urge us to find a solution delamination problem that can be replaced by higher impact tolerance and fracture toughness properties that are incentive when integrated with other methods such as orthogonal 3D woven fabrics. This study looks into a new perspective for analyzing SHM and cure monitoring. Within the purpose of

understanding these new mediums and techniques, three different CNTs and CNCs-based dispersions, CNTs:CNCs-1:2, CNTs:CNCs-1.5:1.5, and CNTs:CNCs-2:1, screen printed onto orthogonal 3D woven glass fiber were studied. The study demonstrated that all inks exhibited shear-thinning behavior within the frequency between 10 s^{-1} to 10^3 s^{-1}. Additionally, the viscosity of the dispersion increased as a result of the addition of CNTs. Different compositions of CNTs:CNCs exhibited varying viscosities and recovery rates, with CNTs:CNCs-2:1 displaying the highest viscosity but facing difficulties passing through the screen printing mold. CNTs:CNCs-1.5:1.5 showed promising results with moderate viscosity and a high recovery rate, allowing for easy transfer onto the surface of woven glass fiber. As the curing cycles progressed, there were noticeable variations in the resistance values of the sensors printed on 3D woven fabrics, effectively capturing the various stages of the process. The cooling stage caused a rise in resistance due to the negative temperature coefficient effect. The results of in-situ compression cycle tests showed that resistance variation varied with different weights, demonstrating the impact of CNTs connection and structural deformation on the composite and conductive line.

ACKNOWLEDGEMENTS

The authors would like to thank TUBITAK 1003 (Project No: 218M703 and 218M704) for supporting this work financially. The authors would like to acknowledge the joint financial support from the Royal Academy of Engineering, UK, and the Scientific and Technological Research Council of Turkey (TÜBİTAK; Project no. 220N307).

REFERENCES

[1] Dwivedi, S. K., Vishwakarma, M., and Soni, P. A. “Advances and Researches on Non Destructive Testing: A Review.” *Materials Today: Proceedings*, Vol. 5, No. 2, 2018, pp. 3690–3698. https://doi.org/10.1016/J.MATPR.2017.11.620.

[2] Zhang, H., Bilotti, E., and Peijs, T. “The Use of Carbon Nanotubes for Damage Sensing and Structural Health Monitoring in Laminated Composites: A Review.” *Nanocomposites*, Vol. 1, No. 4, 2015. https://doi.org/10.1080/20550324.2015.1113639.

[3] Kang, I., Heung, Y. Y., Kim, J. H., Lee, J. W., Gollapudi, R., Subramaniam, S., Narasimhadevara, S., Hurd, D., Kirikera, G. R., Shanov, V., Schulz, M. J., Shi, D., Boerio, J., Mall, S., and Ruggles-Wren, M. “Introduction to Carbon Nanotube and Nanofiber Smart Materials.” *Composites Part B: Engineering*, Vol. 37, No. 6, 2006, pp. 382–394. https://doi.org/10.1016/j.compositesb.2006.02.011.

[4] Siahkouhi, M., Razaqpur, G., Hoult, N. A., Hajmohammadian Baghban, M., and Jing, G. “Utilization of Carbon Nanotubes (CNTs) in Concrete for Structural Health Monitoring (SHM) Purposes: A Review.” *Construction and Building Materials*, Vol. 309, 2021, p. 125137. https://doi.org/10.1016/J.CONBUILDMAT.2021.125137.

[5] Ibanez Labiano, I., Arslan, D., Ozden Yenigun, E., Asadi, A., Cebeci, H., and Alomainy, A. “Screen Printing Carbon Nanotubes Textiles Antennas for Smart Wearables.” *Sensors (Basel, Switzerland)*, Vol. 21, No. 14, 2021. https://doi.org/10.3390/s21144934.

[6] Hu, J., Dun, G., Geng, X., Chen, J., Wu, X., and Ren, T.-L. “Recent Progress in Flexible Micro-Pressure Sensors for Wearable Health Monitoring.” 2023. https://doi.org/10.1039/d2na00866a.

[7] Li, H., Wang, S., Dong, X., Ding, X., Sun, Y., Tang, H., Lu, Y., Tang, Y., and Wu, X. “Recent Advances on Ink-Based Printing Techniques for Triboelectric Nanogenerators: Printable Inks, Printing Technologies and Applications.” *Nano Energy*, Vol. 101, 2022. https://doi.org/10.1016/j.nanoen.2022.107585.

[8] He, P., Cao, J., Ding, H., Liu, C., Neilson, J., Li, Z., Kinloch, I. A., and Derby, B. “Screen-Printing of a Highly Conductive Graphene Ink for Flexible Printed Electronics.” 2019. https://doi.org/10.1021/acsami.9b04589.

[9] Zavanelli, N., and Yeo, W.-H. “Advances in Screen Printing of Conductive Nanomaterials for Stretchable Electronics.” 2021. https://doi.org/10.1021/acsomega.1c00638.

[10] Luo, S., Obitayo, W., and Liu, T. “SWCNT-Thin-Film-Enabled Fiber Sensors for Lifelong Structural Health Monitoring of Polymeric Composites-From Manufacturing to Utilization to Failure.” 2014. https://doi.org/10.1016/j.carbon.2014.04.083.

[11] Lu, S., Chen, D., Wang, X., Shao, J., Ma, K., Zhang, L., Araby, S., and Meng, Q. "Real-Time Cure Behaviour Monitoring of Polymer Composites Using a Highly Flexible and Sensitive CNT Buckypaper Sensor." 2017. https://doi.org/10.1016/j.compscitech.2017.09.025.

[12] Dai, H., and Thostenson, E. T. "Scalable and Multifunctional Carbon Nanotube-Based Textile as Distributed Sensors for Flow and Cure Monitoring." *Carbon*, Vol. 164, 2020, pp. 28–41. https://doi.org/10.1016/j.carbon.2020.02.079.

[13] Yildiz, K., Gürkan, İ., Turgut, F., Cebeci, F., and Cebeci, H. "Fracture Toughness Enhancement of Fuzzy CNT-Glass Fiber Reinforced Composites with a Combined Reinforcing Strategy." *Composites Communications*, Vol. 21, 2020. https://doi.org/10.1016/J.COCO.2020.100423.

[14] Tan, P., Tong, L., Steven, G. P., and Ishikawa, T. "Behavior of 3D Orthogonal Woven CFRP Composites. Part I. Experimental Investigation." *Composites Part A: Applied Science and Manufacturing*, Vol. 31, No. 3, 2000, pp. 259–271. https://doi.org/10.1016/S1359-835X(99)00070-6.

[15] Archer, E., Broderick, J., and McIlhagger, A. T. "Internal Strain Measurement and Cure Monitoring of 3D Angle Interlock Woven Carbon Fibre Composites." *Composites Part B: Engineering*, Vol. 56, 2014, pp. 424–430. https://doi.org/10.1016/j.compositesb.2013.08.067.

[16] Kim, D. H., Kim, S. W., and Lee, I. "Evaluation of Curing Process-Induced Deformation in Plain Woven Composite Structures Based on Cure Kinetics Considering Various Fabric Parameters." *Composite Structures*, Vol. 287, 2022. https://doi.org/10.1016/j.compstruct.2022.115379.

[17] Blanco, S., You, H., Kerekes, T. W., and Yun, G. J. "Cure-Induced Residual Stress Buildup and Distortions of CFRP Laminates with Stochastic Thermo-Chemical and Viscoelastic Models: Experimental Verifications." *Mechanics of Advanced Materials and Structures*, Vol. 29, No. 19, 2022, pp. 2740–2756. https://doi.org/10.1080/15376494.2021.1877376.

[18] Shariatnia, S., Kumar, A. V., Kaynan, O., Asadi, A., Asadi, A., and Asadi, A. "Hybrid Cellulose Nanocrystal-Bonded Carbon Nanotubes/Carbon Fiber Polymer Composites for Structural Applications." *ACS Applied Nano Materials*, Vol. 3, No. 6, 2020, pp. 5421–5436. https://doi.org/10.1021/acsanm.0c00785.

[19] Liu, L., Shen, Z., Zhang, X., and Ma, H. "Highly Conductive Graphene/Carbon Black Screen Printing Inks for Flexible Electronics." *Journal of Colloid and Interface Science*, Vol. 582, 2021, pp. 12–21. https://doi.org/10.1016/j.jcis.2020.07.106.

[20] Luo, S., Wang, G., Wang, Y., Xu, Y., and Luo, Y. "Carbon Nanomaterials Enabled Fiber Sensors: A Structure-Oriented Strategy for Highly Sensitive and Versatile in Situ Monitoring of Composite Curing Process." *Composites Part B: Engineering*, Vol. 166, 2019, pp. 645–652. https://doi.org/10.1016/j.compositesb.2019.02.067.

[21] Luo, S., Obitayo, W., and Liu, T. "SWCNT-Thin-Film-Enabled Fiber Sensors for Lifelong Structural Health Monitoring of Polymeric Composites - From Manufacturing to Utilization to Failure." *Carbon*, Vol. 76, 2014, pp. 321–329. https://doi.org/10.1016/J.CARBON.2014.04.083.

[22] Lu, S., Zhao, C., Zhang, L., Chen, D., Chen, D., Wang, X., and Ma, K. "Real Time Monitoring of the Curing Degree and the Manufacturing Process of Fiber Reinforced Composites with a Carbon Nanotube Buckypaper Sensor." *RSC Advances*, Vol. 8, No. 39, 2018, pp. 22078–22085. https://doi.org/10.1039/c8ra03445a.